Materials Today: Proceedings 38 (2021) 2890–2898

Contents lists available at ScienceDirect

Materials Today: Proceedings

journal homepage: www.elsevier.com/locate/matpr

Numerical modelling of bonded and unbonded flax fiber reinforced elastomeric isolator and their application to RC building

Saiteja Sistla *, Mohan S.C.

BITS Pilani Hyderabad Campus, 500078, India

ARTICLE INFO

Article history:
Received 28 March 2020
Received in revised form 25 August 2020
Accepted 4 September 2020
Available online 20 October 2020

Keywords:
Fibre reinforced elastomeric isolator
Reinforced concrete buildings
Passive seismic protection
Finite element modelling
Earthquake engineering

ABSTRACT

Earthquakes are natural disasters causing havoc to life and property since several centuries. Indian subcontinent has a history of devastating earthquakes in its recent past. One way to tackle an earthquake is to equip the building with a proper seismic resistant system. One of the most popular and effective technique for low and midrise buildings is base isolation. However, existing base isolation systems are very expensive for non-commercial buildings. Hence, this study mainly concentrates on fibre reinforced elastomeric isolators which are cost efficient without a marginal compromise in its performance. A comparison between the performance of unbonded and bonded fibre reinforced elastomeric isolators has been carried out. The unbonded fibre reinforced elastomeric isolators have better performance in terms of stresses, horizontal flexibility, and damping. A low rise reinforced concrete residential building's response is studied with and without fibre reinforced elastomeric isolators. The results show significant reduction in storey drift, story shear, storey level acceleration in both equivalent static method and time history analysis, along with increase in the time period of building's fundamental mode.

1. Introduction

India has experienced few severe earthquakes like Koyna (1967), Latur (1993), Bhuj (2001) etc. in the last century. More than 50% area in India is highly prone to earthquakes. From estimations, the Himalayan region can probably experience earthquake magnitude greater than 8.0 in the future [1]. The main reason for the high intensity and frequency of earthquakes in the north eastern part maybe due to the upliftment of tectonic plates at the rate of two to twelve mm per year in the Himalayan region approximately [2]. Base isolators have become quite popular under passive seismic protection in the past few decades. This technique is often applied to mid-rise buildings and involves heavy expenditure. When it comes to low rise buildings which constitute to majority of the buildings in India, economy of the seismic protection device without any compromise in its performance is very crucial. The two main properties of a good base isolator are high vertical stiffness and horizontal flexibility. The vertical stiffness ensures safe transfer of vertical loads on the other hand horizontal flexibility is the main component that increases the time period of the building which helps in response reduction. Conventional base isolation devices consist of alternate layers of steel plate and rubber. The steel-rubber bond restrains the lateral expansion of rubber when vertical load is acting and hence leading to high vertical stiffness. Conventional isolators are heavy and their expense is about 50–60% of the construction cost of the building [3]. Hence, fibre reinforced elastomeric isolator (FREI) is an alternative for the conventional isolation systems in terms of economy and performance for low rise buildings [4]. The FREI is like conventional isolation system where the steel plates are replaced by fibre reinforcement making them lighter and easy to manufacture. The FREI are further classified into two types i.e. unbonded and bonded FREI. Kelly and Takhirov [5] extensively worked on the experimental investigation of FREI and its application. They have experimentally tested FREI of various shapes such as circular, square, rectangular to estimate their performance in terms of vertical stiffness, horizontal stiffness, and viscous damping. Mathematical equations developed by Kelly and Takhirov are used to design the isolation system in this study. Habieb et al. [6] have utilized rubber of shore A hardness equal to

* Corresponding author.
E-mail address: h20181430050@hyderabad.bits-pilani.ac.in (S. Sistla).

https://doi.org/10.1016/j.matpr.2020.09.143
2214-7853/

40 with an approximate damping of 10–12%, to develop an unbonded fibre reinforced elastomeric isolation (UFREI) system applied to a masonry structure. To ease the implementation and modelling of UFREI in ABAQUS, Habieb et al. [7] have developed user subroutine to predict the behaviour of UFREI under seismic loading. Thuyet et al. [8] have fabricated and used 14 UFREI to isolate a two storeyed masonry building in Tawang, India. As a part of their study they have experimentally tested and numerically simulated UFREI subjected to ground excitation. In another interesting research, Thuyet et al. [9] have estimated the horizontal stiffness of UFREI by developing a mathematical model which is in strong agreement with the experimental results. Mishra et al. [10] have effectively used scrap rubber tyre for fabrication of FREI and tested it experimentally and analytically. Scrap rubber tyre is reinforced with fibre, making it one of the cheapest solutions for base isolation. Sierra et al. [11] have experimentally tested circular FREI and used it to isolate a five storeyed building. An interesting outcome of their research is the determination of failure mode of circular UFREI experimentally. Calabrese et al. [12] have developed hysteresis models for recycled rubber fibre reinforced bearings (RR-FRB). They have used a bilinear hysteresis model which agrees with the experimental results to represent base isolation of a scaled steel frame model. Engelen et al. [13] have numerically evaluated the performance of partially bonded FREI (PB-FREI) used as bridge bearings. A bilinear Takeda model is implemented by the authors to represent the behaviour of PB-FREI and to evaluate its seismic isolation efficiency in OpenSees software. The above-mentioned research was mainly oriented towards base isolation of masonry structures using FREI. Present study concentrates on numerical modelling and application of UFREI with locally available flax fibre to a reinforced concrete building. A finite element package, ABAQUS [14] is used to evaluate the performance UFREI, bonded fibre reinforced elastomeric isolator (BFREI) to obtain the stiffness and damping properties which will further be used as an input in ETABS [15]. Reinforced concrete building is modelled, with and without FREI and analysed for their performance under seismic forces by using equivalent static and time history methods. The results show improved seismic resistant behaviour of the building with UFREI which will be discussed further in the sections below.

2. Numerical validation

It is essential to validate the finite element model with an experimental model in order to ensure the authenticity of the modelling procedure adopted. Nezhad et al. [16] have experimentally evaluated the performance of square carbon fibre reinforced elastomeric isolators. The validated results and elevation of the isolator modelled are shown in Figs. 1, 2.

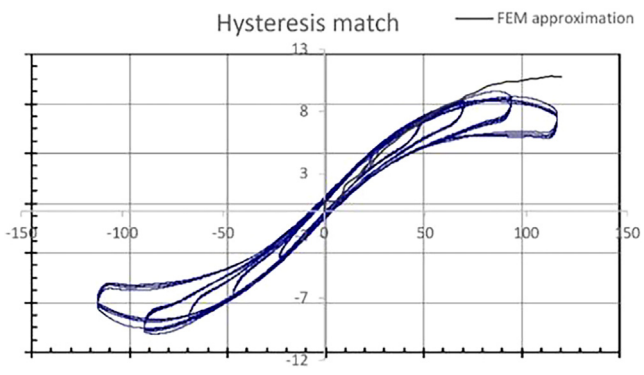

Fig. 1. Numerical Validation.

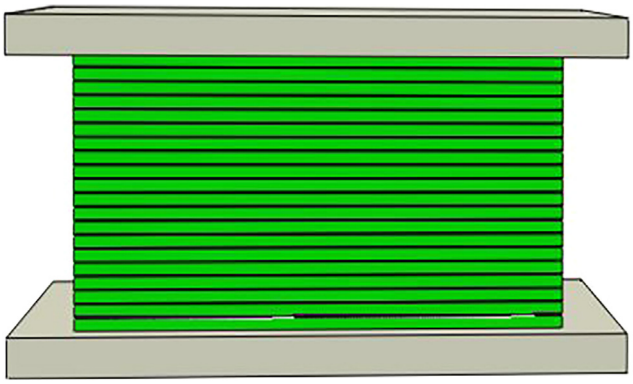

Fig. 2. Carbon fiber reinforced isolator.

In Fig. 2 grey coloured elements represent the loading plates, green coloured elements represent the rubber, black coloured elements represent the fibre. The hyper elastic properties of the rubber were only available and hence the unloading path remains the same as that of the loading path. Along with the numerical validation, mesh sensitivity analysis was carried out for sizes of 11 mm, 9 mm, 7 mm and 5 mm respectively. As the mesh size was varied from 11 mm to 5 mm, there was a variation in the results yielded by the models. Although there were very minute changes in the stress distribution when the mesh size was reduced from 7 mm to 5 mm, it was not significant and hence a mesh size of 7 mm is adopted.

3. Material properties

Unbonded fibre reinforced elastomeric isolators consists of alternate layers of rubber and fibre bonded together. The two main properties of rubber are hyper elasticity and viscoelasticity. Hyper elasticity is essential for the isolation system to undergo large strains without yielding, whereas visco elasticity is important for energy dissipation. Yeoh's hyper elasticity model [17], Prony series [18] are used to evaluate the hyper and visco elastic properties of rubber [7] as shown in Tables 1, 2.

It is observed that the fibre stresses are low and they remain in the elastic range. The current study involves the usage of flax fibre commonly known as flax or linseed. It is a food/fibre crop mostly cultivated in cold climatic conditions. The approximate cost of the fibre is around 150 rs/kg. The elastic properties of the fibre [19] are mentioned in Table 3.

4. Modelling and simulation

A two storeyed reinforced concrete building plan shown in Fig. 3, located in Indian seismic zone V is used for this study. Gravity load analysis and design was carried out on ETABS where the members were safe during gravity load design. Building and loading details are mentioned in the Table 4.

4.1. ABAQUS modelling

The numerical simulation of FREI is carried out using ABAQUS software to obtain the vertical stiffness, horizontal stiffness and viscous damping of the isolator to be used under the building. The dimensions of UFREI and BFREI are calculated according to equations mentioned in previous literature [4] and shown in Table 5. The material properties essential for numerical modelling are provided in Table 1–3. The isolator is subjected to 60 mm peak horizontal cyclic displacement with corresponding amplitude

Table 1
Hyper elastic properties of rubber.

C_{10} (MPa)	C_{20} (MPa)	C_{30} (MPa)	D_1	D_2	D_3
0.2551	0.0066	0.000032	0.00218	8.68E−05	−1.794E−05

Table 2
Viscoelastic properties.

g	0.333	0.333
T (s)	0.04	100

Table 3
Elastic properties of fiber.

E (MPa)	μ
50,000	0.23

Table 4
Building properties and loading details.

Description	Details
Grade of concrete	M20
Grade of steel	Fe415
Beam size	240 × 240 mm
Column size	270 × 300 mm
Number of columns	17
Slab thickness	100 mm
Live load	1 KN/m^2
Wall load	8 KN/m
Seismic zone [India]	V
Soil type	Medium
Fundamental time period	0.58 s
Target response spectrum	IS:1893 Part 1 [20]

factor shown in Fig. 4. To simulate the building load, a vertical pressure of 3 N/mm^2 is applied on the top plate. The boundary conditions used for modelling and simulation of FREI are shown in Table 6.

4.2. Numerical simulation

The unbonded and bonded FREI are modelled with same dimensions using equal quantity of rubber and fibre. There is an addi-

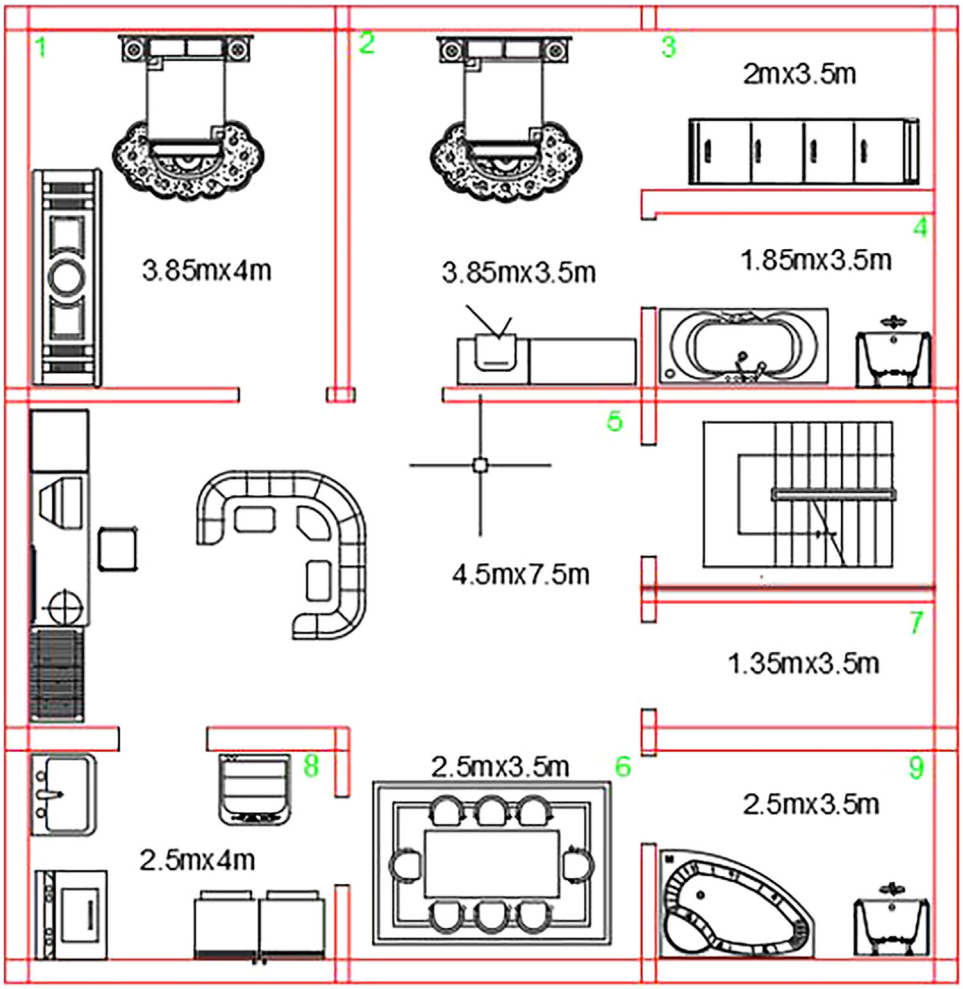

Fig. 3. Plan of two storeyed RC building.

Table 5
Isolator dimensions and loading details.

Description	Value
Load on each isolator	6116.2 kgs
Length of isolator	200 mm
Breadth of isolator	100 mm
Depth of isolator	52 mm
Pressure on isolator	3 N/mm^2
No. of rubber layers	5
Thickness of one rubber layer	10 mm
Number of fibre layers	4
Thickness of one rubber layer	0.5 mm

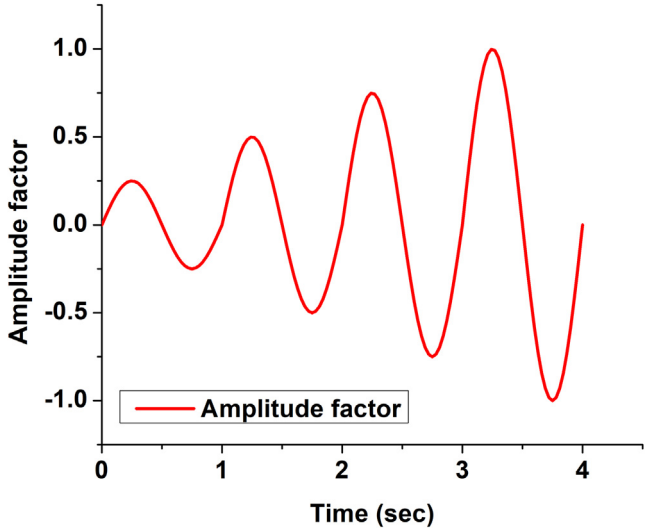

Fig. 4. Amplitude factor vs Time.

Table 6
Boundary conditions.

	Description	Boundary condition
BFREI	Rubber and fibre	Tie constraint
	Rubber and top plate	Tie constraint
	Rubber and bottom plate	Tie constraint
UFREI	Rubber and fibre	Tie constraint
	Rubber and top plate	μ = 0.85 (penalty friction)
	Rubber and bottom plate	μ = 0.85 (penalty friction)
Both the cases	Bottom plate	Restrained against movement
	Top plate	Displacement – 60 mm amplitude

tional requirement of top and bottom steel plates in the case of BFREI, where UFREI can be directly placed under the building. The main agenda of this simulation is to obtain the vertical stiffness, horizontal stiffness and hysteresis loop of the isolators. The variation in stress distribution of BFREI and UFREI loaded along the shorter direction is shown in Fig. 5a and b. The loading along shorter, longer and diagonal direction are represented by 90 °, 0°, 45 ° respectively. From the stress distribution pattern seen in Fig. 5a and b it is quite evident that the stresses in rubber are higher by 25% in the BFREI case when compared to that of UFREI. "Troubleshooting Finite-Element Modeling with Abaqus with Application in Structural Engineering Analysis" [21] was very helpful in dealing with the errors occurred during modelling and simulation. The hysteresis plots for UFREI and BFREI are shown in Fig. 6 respectively. Based on these hysteresis plots, isolator properties are evaluated in Section 4.3.

4.3. Evaluation of vertical, horizontal stiffness and damping of FREI

The equations used to compute the effective horizontal stiffness, equivalent viscous damping ratio from hysteresis loop are adopted from [4], which can be used for both BFREI and UFREI.

$$K_{eff}^{h} = \frac{F_{max} - F_{min}}{d_{max} - d_{min}} \tag{1}$$

$$\beta = \frac{W_d}{4\pi W_s} \tag{2}$$

$$W_s = \frac{K_{eff}^{h}(\Delta\max)^2}{2} \tag{3}$$

$$\Delta_{\max} = \frac{d_{max} + d_{min}}{2} \tag{4}$$

where, F_{max} is the maximum force from the hysteresis loop, F_{min} is minimum force from the hysteresis loop, d_{max} is the maximum displacement from the hysteresis loop, d_{min} is the minimum displacement from the hysteresis loop, β is the equivalent viscous damping ratio, K_{eff}^{h} is the effective horizontal stiffness, W_s is the energy stored or elastic energy, W_d is the energy dissipated i.e. area of the hysteresis loop. The effective horizontal stiffness and equivalent damping ratio of BFREI and UFREI for 60 mm cycle displaced in different directions are summarized in Table 7. The UFREI has lower horizontal stiffness i.e. high horizontal flexibility when compared to that of BFREI due to the reduction of contact area with increasing horizontal displacement. Wider hysteresis loops indicate higher viscous damping and hence UFREI has higher damping when compared to BFREI.

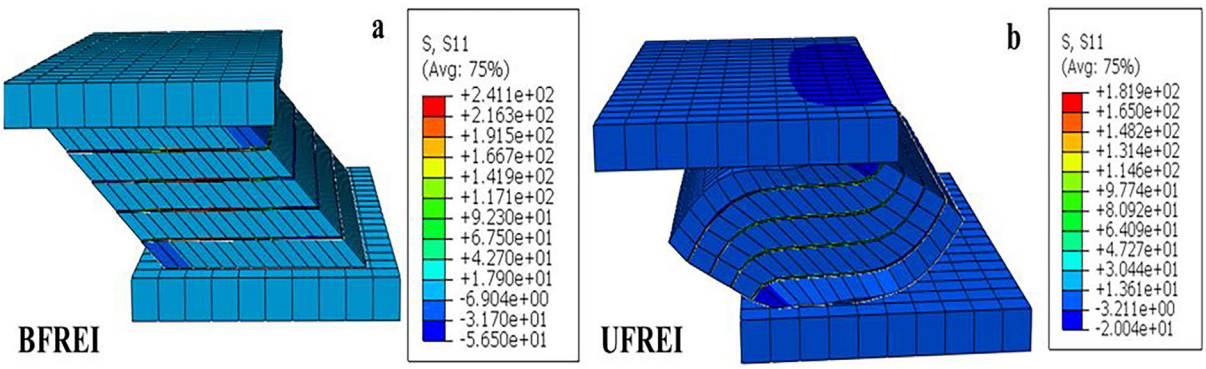

Fig. 5. a, b Stress distribution along x direction (S_{11}) of BFREI and UFREI.

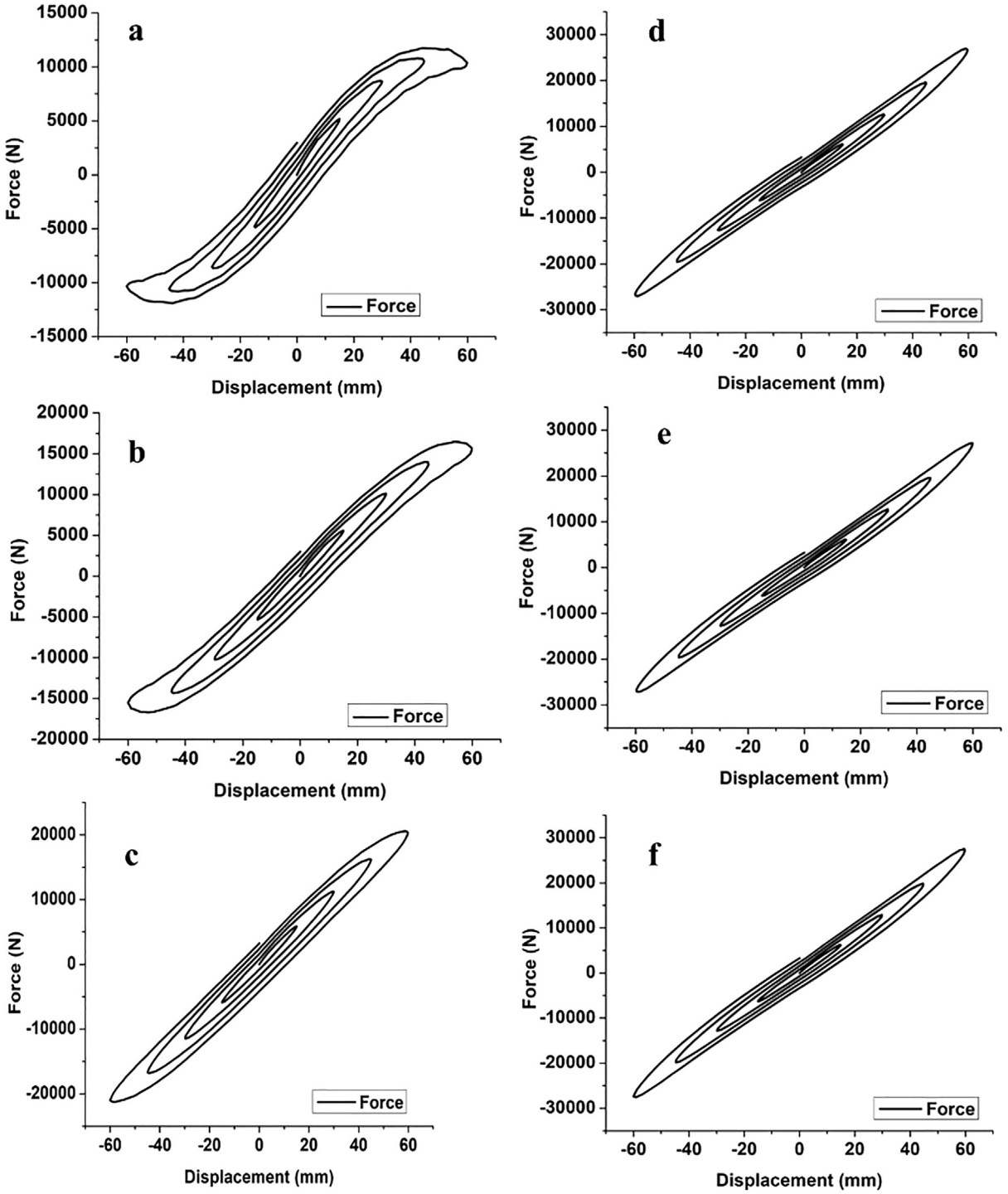

Fig. 6. (a)-(c) Unbonded 90°, 45°, 0° Hysteresis plot (d)-(f) Bonded 90°, 45°, 0° Hysteresis plot.

Table 7
Summary of hysteresis loop of FREI displaced in different directions.

Isolator type	F_{max}	F_{min}	d_{max}	d_{min}	K^h_{eff}	β
UFREI 90 °	11,748	−11914.4	59.9	−60	197.44	10.93
UFREI 45 °	16460.8	−16678	59.99	−59.99	276.66	9.45
UFREI 0°	18,770	−18823.8	59.8	−60	313.81	8.88
BFREI 90 °	26933.4	−27031.1	59.74	−59.84	451.60	6.27
BFREI 45 °	27117.9	−27146.1	59.81	−59.74	453.87	6.34
BFREI 0 °	27497.5	−27566	59.79	−59.96	460.03	6.36

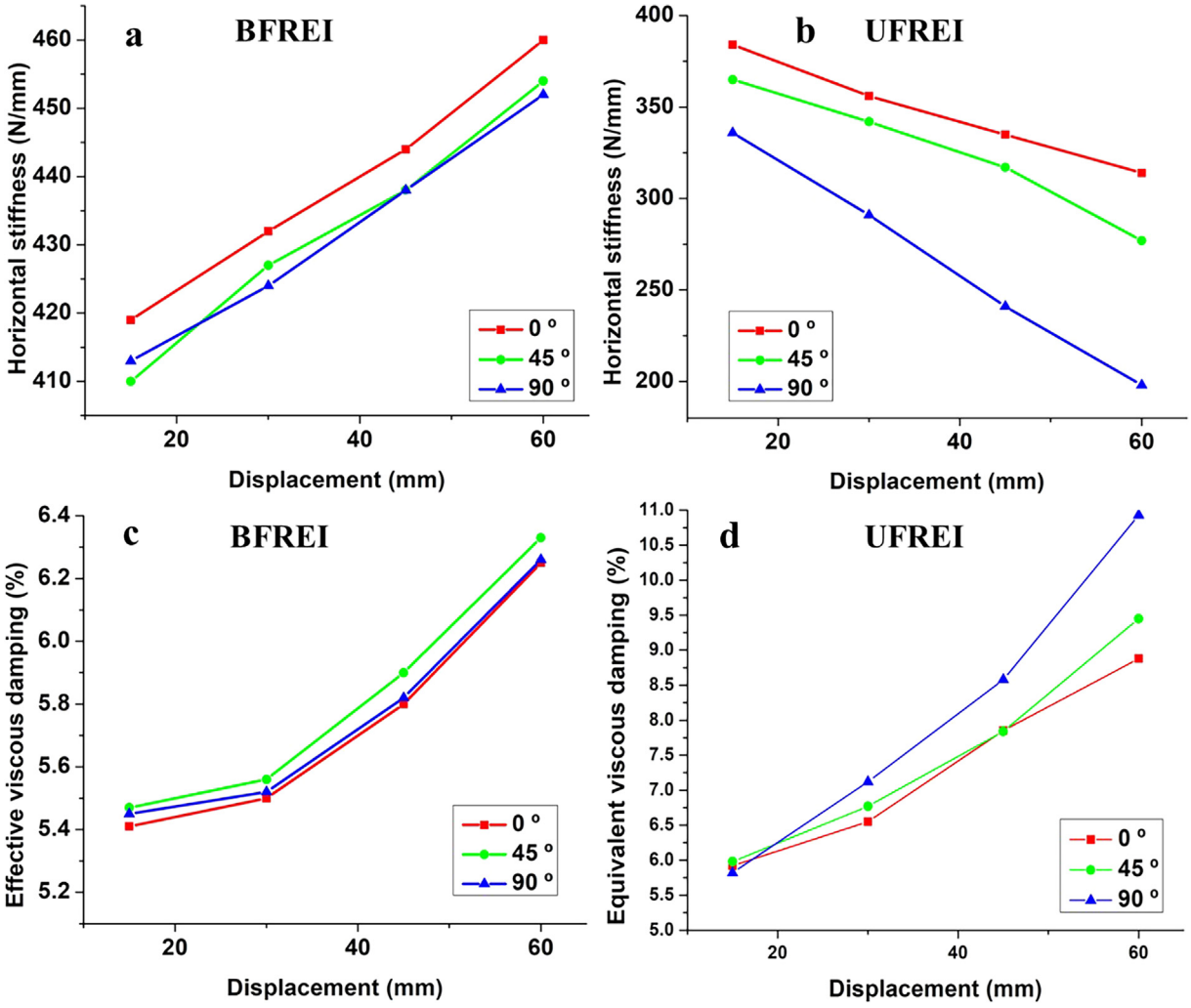

Fig. 7. Comparison of (a), (b) Horizontal stiffness, (b), (d) Equivalent damping ratio obtained from hysteresis.

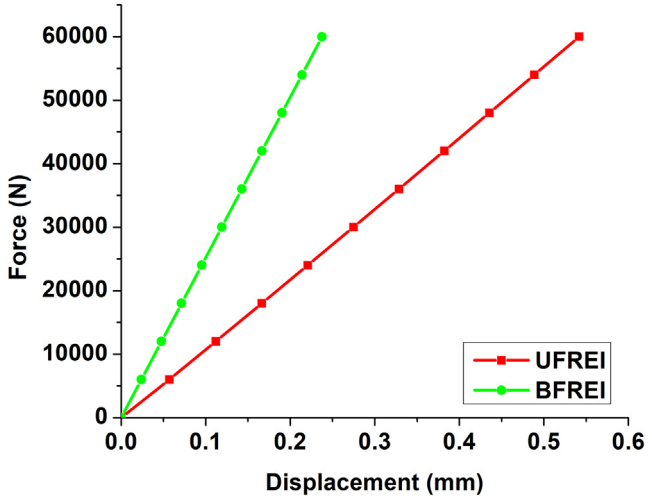

Fig. 8. FREI Vertical load – Deflection plot.

Table 8
Earthquakes used for time history analysis.

Earthquake	Year
Corralitos	1923
Kocaeli	1999
ChiChi	1999
Loma prieta	1989

A detailed comparison of horizontal stiffness, equivalent viscous damping ratio for increasing displacement along different loading directions are shown in Fig. 7. Qualities of a good isolator mainly include low horizontal stiffness and high damping capability. The stiffness is found to be reducing with increasing displacement for UFREI while vice versa has been observed for BFREI as seen in Fig. 7a, b respectively. Increasing trend of equivalent viscous damping was observed in both the cases while the UFREI has higher damping as seen in Fig. 7c, d. By understanding the

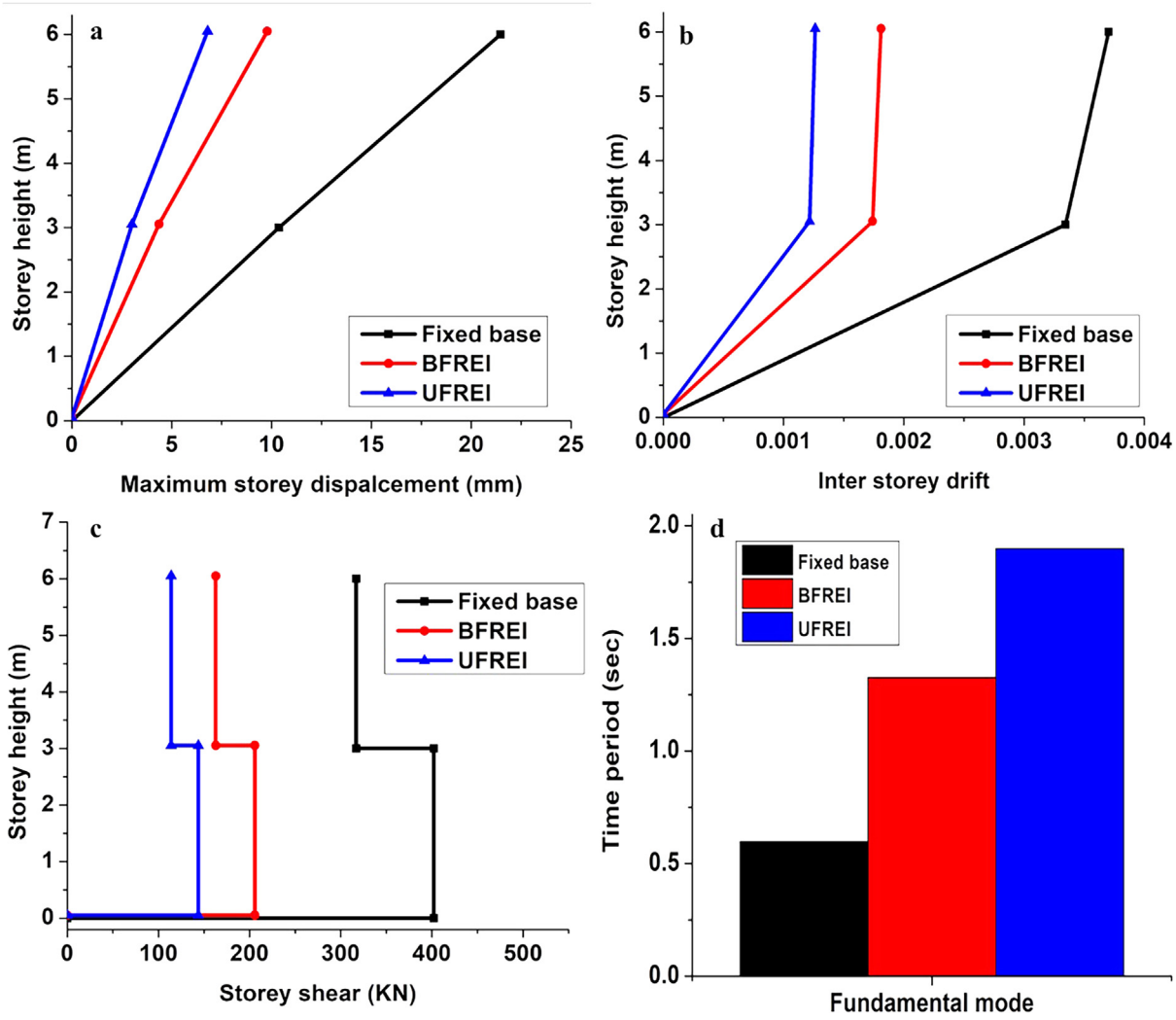

Fig. 9. Performance comparison of UFREI and BFREI by equivalent static method.

results, it can be inferred that UFREI is performing better than BFREI in terms of required horizontal flexibility and damping.

Furthermore, the vertical stiffness of UFREI and BFREI are evaluated and compared as shown in Fig. 8. This represents the vertical stiffness of FREI only due to the application of factored weight of the building and live load. It is observed that BFREI has better vertical stiffness due to its restraint in terms of bonding when compared to that of UFREI.

5. Application of UFREI and BFREI

The seismic performance of two storeyed building isolated with BFREI and UFREI is evaluated using equivalent static method and linear time history analysis for four different earthquakes (Table 8) scaled to match the Indian target response spectrum. The main parameters required for modelling the base isolation system in ETABS, such as vertical, horizontal stiffness and equivalent viscous damping coefficient, are derived in the previous section. The representation of these properties in ETABS is facilitated through link elements. A multi linear plastic link element is used to represent the isolation systems in this study. The results of the equivalent static analysis are presented in Fig. 9.

The maximum top storey displacement of the fixed base building exceeds the allowable limit by 12% [20]. The building isolated with UFREI and BFREI has yielded favourable results such as reduction of maximum top storey displacement by 54% and 68%, inter storey drift by 51% and 65% and base shear by 48% and 64% as seen in Fig. 9a–c respectively. The reduction in seismic demand is usually efficient if the fundamental time period of an isolated building is at least 3 times greater than that of a fixed base building. The former criterion is satisfied by UFREI system while BFREI system failed to do so as seen in Fig. 9d.

Furthermore, dynamic analysis is carried out to evaluate the performance of BFREI and UFREI under actual earthquake time history scaled to Indian target response spectrum, zone V, medium soil. The results of linear time history analysis in terms of top storey displacement is shown in Fig. 10. As observed in static analysis, similar trend is followed in terms of seismic performance. The average reduction in top storey displacement from four different time history analysis is 41% and 60% for BFREI and UFREI respectively.

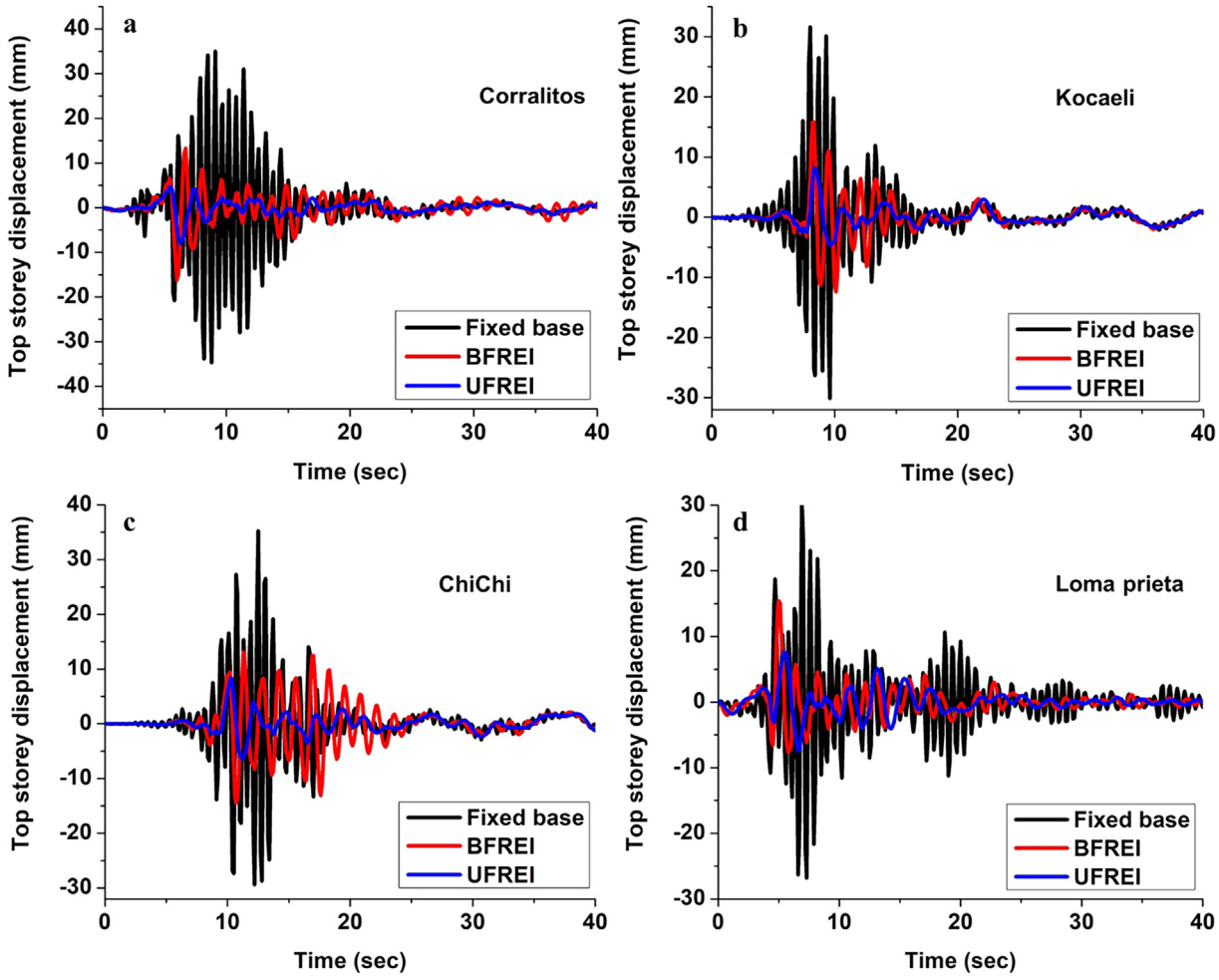

Fig. 10. Performance comparison of UFREI and BFREI by time history analysis.

Table 9
Summary of time history analysis results.

Earthquake	V^F_{max}KN	V^B_{max}KN	V^U_{max}KN	A^F_{max}m/s^2	A^B_{max}m/s^2	A^U_{max}m/s^2
Corralitos	650	382	249	4.94	2.2	1.5
Kocaeli	714	385	259	3.5	2.5	2.1
ChiChi	703	354	231	4.36	2.2	1.6
Loma prieta	632	382	240	3.2	1.9	1.5

V^F_{max} Absolute maximum base shear of fixed base building
V^B_{max} Absolute maximum base shear of BFREI building
V^U_{max} Absolute maximum base shear of UFREI building
A^F_{max} Absolute maximum acceleration of fixed base building
A^B_{max} Absolute maximum acceleration of BFREI building
A^U_{max} Absolute maximum acceleration of UFREI building

Important seismic performance parameters of building such as maximum base shear and maximum acceleration at the top storey level are presented in Table 9. Average reduction of base shear by 44% and 63.6% and top storey acceleration by 43.5% and 56.5% are observed for BFREI and UFREI respectively.

UFREI being flexible, allows higher displacement at the isolator level and greater time period separation as seen in Fig. 11. Hence, UFREI system is more efficient compared to BFREI of equal dimensions in improving the seismic performance of two storeyed RC building subjected to various earthquakes.

6. Conclusions

Investigation of fibre reinforced elastomeric isolators as an application to a low-rise RC building is carried out in this study. Finite element analysis of unbonded and bonded FREI is carried out to obtain their vertical stiffness, effective horizontal stiffness, and equivalent viscous damping ratio. The seismic performance of FREI to isolate building subjected to various ground motions is studied and key findings are summarized below:

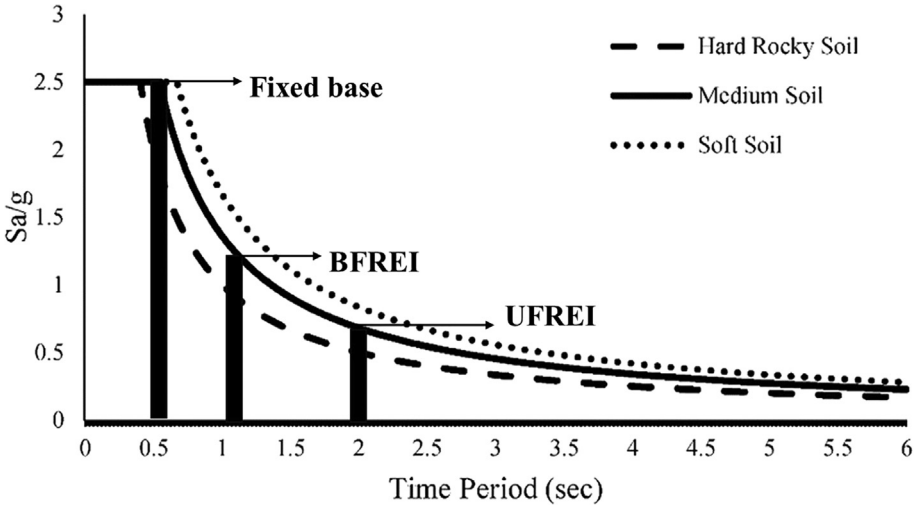

Fig. 11. Natural time period separation of fundamental mode for different buildings.

1. The horizontal flexibility and damping capability of UFREI is higher than BFREI of same dimensions and material properties. The stress distribution of UFREI is significantly lower allowing roll over phenomenon unlike BFREI.
2. High vertical stiffness is essential to withstand the weight of the building and avoid potential rocking motion. The vertical to horizontal stiffness ratio is higher than 150 for UFREI and BFREI according to Eurocode 8 [22] and hence they are suitable for base isolation.
3. The reduction in top storey displacement, storey shear is higher for the building isolated with UFREI, as evident from both equivalent static and time history analysis. Furthermore, the maximum top storey acceleration is significantly reduced by UFREI compared to BFREI.
4. The better seismic performance of UFREI is attributed to its capability to achieve higher time period separation and damping there by reducing the overall seismic demand on the building.

CRediT authorship contribution statement

Saiteja Sistla: Conceptualization, Methodology, Writing - original draft, Writing - review & editing, Software. **S.C. Mohan:** Investigation, Visualization.

Declaration of Competing Interest

The authors declare that they have no known competing financial interests or personal relationships that could have appeared to influence the work reported in this paper.

References

[1] S.K. Jain, Indian earthquakes: an overview, Indian Concr. J. 72 (1998) 555–561.
[2] S. Chatterjee, A. Goswami, C.R. Scotese, The longest voyage: Tectonic, magmatic, and paleoclimatic evolution of the Indian plate during its northward flight from Gondwana to Asia, Gondwana Res. 23 (1) (2013) 238–267.
[3] V. Kilar, S. Petrovčič, D. Koren, S. Šilih, Cost viability of a base isolation system for the seismic protection of a steel high-rack structure, Int. J. Steel Struct. 13 (2) (2013) 253–263.
[4] J.M. Kelly, S.M. Takhirov, Analytical and Experimental Study of Fiber-Reinforced Elastomeric Isolators Fiber-Reinforced Elastomeric Isolators, Rep. No. PEER 2001/11, Pacific Earthq. Eng. Res. Center, Univ. California, Berkeley., 2001.
[5] J.M. Kelly, A. Calabrese, Pacific Earthquake Engineering Mechanics of Fiber Reinforced Bearings, (2012).
[6] A.B. Habieb, G. Milani, Tavio, F. Milani, Low cost rubber seismic isolators for masonry housing in developing countries, AIP Conf. Proc. 1906 (2017) 664–670, https://doi.org/10.1063/1.5012369.
[7] Ahmad Basshofi Habieb, Marco Valente, Gabriele Milani, Implementation of a simple novel Abaqus user element to predict the behavior of unbonded fiber reinforced elastomeric isolators in macro-scale computations, Bull. Earthquake Eng. 17 (5) (2019) 2741–2766.
[8] V.N. Thuyet, S.K. Deb, A. Dutta, Mitigation of Seismic Vulnerability of Prototype Low-Rise Masonry Building Using U-FREIs, 32 (2018) 1–13. https://doi.org/10.1061/(ASCE)CF.1943-5509.0001136.
[9] Thuyet Van Ngo, Anjan Dutta, Sajal K. Deb, Evaluation of horizontal stiffness of fibre-reinforced elastomeric isolators: Evaluation of Horizontal Stiffness of FREIs, Earthquake Eng. Struct. Dyn. 46 (11) (2017) 1747–1767.
[10] Huma Kanta Mishra, Akira Igarashi, Hiroshi Matsushima, Finite element analysis and experimental verification of the scrap tire rubber pad isolator, Bull. Earthquake Eng. 11 (2) (2013) 687–707.
[11] Ingrid E. Madera Sierra, Daniele Losanno, Salvatore Strano, Johannio Marulanda, Peter Thomson, Development and experimental behavior of HDR seismic isolators for low-rise residential buildings, Eng. Struct. 183 (2019) 894–906.
[12] A. Calabrese, M. Spizzuoco, S. Strano, M. Terzo, Hysteresis models for response history analyses of recycled rubber–fiber reinforced bearings (RR-FRBs) base isolated buildings, Eng. Struct. 178 (2019) 635–644.
[13] Niel C. Van Engelen, Michael J. Tait, Peyman M. Osgooei, Partially bonded fiber-reinforced elastomeric isolators (PB-FREIs), Struct. Control Heal. Monit. (2014), https://doi.org/10.1002/stc.
[14] Abaqus 6.11, Reference manual.
[15] ETABS Tutorial ETABS ®, Reference manual.
[16] T. Nezhad, Hamid & Tait, Michael & Drysdale, Robert, Testing and modeling of square carbon fiber-reinforced elastomeric seismic isolators, Struct Control Health Monitor. (200815. 876 - 900. 10.1002/stc.225.
[17] O.H. Yeoh, Some forms of the strain energy function for rubber, Rubber Chem. Technol. 66 (1993) 754–771. https://doi.org/10.5254/1.3538343.
[18] T. Chen, Determining Viscoelastic Strain Data a Prony Material Series for a From Time Varying, Nasa. (2000) 26.
[19] A. Mohajerani, S.Q. Hui, M. Mirzababaei, A. Arulrajah, S. Horpibulsuk, A.A. Kadir, M.T. Rahman, F. Maghool, Amazing types, properties, and applications of fibres in construction materials, Materials (Basel). 12 (2019) 1–45, https://doi.org/10.3390/ma12162513.
[20] Criteria for Earthquake Resistant Design of Structures, IS: 1893, 2016.
[21] R.J. Boulbes, Troubleshooting Finite-Element Modeling with Abaqus, 2020. https://doi.org/10.1007/978-3-030-26740-7.
[22] Eurocode 8: Design of structures for earthquake resistance - Part 1 : General rules, seismic actions and rules for buildings, EN 1998-1, 2004.